

First-principles study of roles of Cu and Cl in polycrystalline CdTe

Ji-Hui Yang,¹ Wan-Jian Yin,^{1,2} Ji-Sang Park,¹ Wyatt Metzger,¹ and Su-Huai Wei^{1,3,a)}

¹National Renewable Energy Laboratory, Golden, Colorado 80401, USA

²College of Physics, Optoelectronics and Energy and Collaborative, Innovation Center of Suzhou Nano Science and Technology, Soochow University, Suzhou 215006, China

³Beijing Computational Science Research Center, Beijing 100094, China

(Received 16 December 2015; accepted 12 January 2016; published online 25 January 2016)

Cu and Cl treatments are important processes to achieve high efficiency polycrystalline cadmium telluride (CdTe) solar cells, thus it will be beneficial to understand the roles they play in both bulk CdTe and CdTe grain boundaries (GBs). Using first-principles calculations, we systematically study Cu and Cl-related defects in bulk CdTe. We find that Cl has only a limited effect on improving p-type doping and too much Cl can induce deep traps in bulk CdTe, whereas Cu can enhance p-type doping of bulk CdTe. In the presence of GBs, we find that, in general, Cl and Cu will prefer to stay at GBs, especially for those with Te-Te wrong bonds, in agreement with experimental observations. © 2016 AIP Publishing LLC. [<http://dx.doi.org/10.1063/1.4940722>]

I. INTRODUCTION

Cadmium telluride (CdTe) is the leading thin-film solar cell material for low-cost, high-efficiency photovoltaic (PV) applications and it has been extensively studied during the past half century. Its advantages as a solar cell absorber include its high optical absorption coefficient and a direct bandgap of 1.5 eV that is nearly ideal for optimal solar conversion. Recently, First Solar has achieved a world-record cell efficiency of 21.5%.¹

Experimentally, it is well known that both Cu and Cl treatments are crucial to obtain high energy conversion efficiencies. However, the exact roles of Cu and Cl in enhancing and even limiting CdTe solar cell efficiency are still under debate as many explanations and mechanisms have been proposed. For example, research has indicated that Cl improves grain growth and recrystallization,^{2,3} enhances S diffusion from CdS to CdTe,^{4,5} passivates deep defect levels within the band gap,^{2,6,7} and helps current collection.^{8–11} Although Cl incorporation does improve polycrystalline CdTe solar cell efficiency, studies on single-crystal CdTe indicate that too much Cl will induce hole traps deep in the middle of the CdTe bandgap, thereby limiting the solar cell performance.^{8,12} The fact that the CdCl₂ treatment is only necessary in polycrystalline CdTe but not in single crystals suggests that Cl may have strong interactions with CdTe grain boundaries (GBs). For Cu, the common perception in this field is that the role of Cu is to reduce the back contact barrier,^{13,14} enhance p-type doping in CdTe, and modify lifetime.^{15–17} However, Cu is also mobile, and this can affect doping and the back contact quality during operation, leading to stability issues.^{18,19}

Due to the important roles that Cl and Cu play in CdTe solar cells, it will be of great interest to understand the following questions: (1) What kind of defects Cl can form in bulk CdTe and do these lead to the deep levels as observed in Refs. 8 and 12? (2) How does Cl interact with CdTe

grain boundaries? (3) Why can Cu enhance p-type doping in bulk CdTe and how does Cu interact with CdTe grain boundaries?

To answer these questions, we use first-principles calculations to study both Cl and Cu-related defects in bulk CdTe and their segregation at CdTe grain boundaries. We find that although the A center ($Cl_{Te} + V_{Cd}$) formed by Cl has a shallow acceptor level close to the valence band maximum (VBM), it has a high formation energy once all the Cd vacancies are consumed. As a result, Cl has a limited effect on improving p-type doping in bulk CdTe related to Cd vacancy concentration. When more Cl is introduced, the donor defects Cl_i^+ and Cl_{Te}^+ and the acceptor defect Cl_i^- will strongly compensate each other with a deep level at about 0.75 eV above the VBM, in agreement with the observations in Refs. 8 and 12. For Cu doping, the substitutional defect Cu_{Cd} has a calculated acceptor level at 0.16 eV above the VBM. This is in agreement with the experimental studies which indicate that Cu_{Cd} acceptor level is 0.146 eV above the VBM.²⁰ Compared with our recently calculated Cd vacancy level at 0.36 eV, it implies that Cu can enhance p-type doping in bulk CdTe. For Cu and Cl interactions with CdTe GBs, we find that Cl and Cu generally prefer to segregate at GBs, especially those with Te-Te wrong bonds like Te-core $\Sigma 3(112)$ GB except negatively charged Cu_{Cd}. We expect that our findings can help to understand Cl and Cu behaviors in polycrystalline CdTe and thus contribute to further improving CdTe solar technology.

II. FIRST-PRINCIPLES CALCULATION METHODS

Our first-principles total-energy and band-structure calculations are performed using density-functional theory (DFT)^{21,22} as implemented in the VASP code.^{23,24} The electron and core interactions are included using the frozen-core projected augmented wave (PAW) approach.²⁵ To correct the bandgap error, we used the Heyd-Scuseria-Ernzerhof (HSE06) hybrid functional.²⁶ The bulk defect calculations are performed using the scheme described in Ref. 27 within

^{a)}Email: suhuaiwei@csrsc.ac.cn

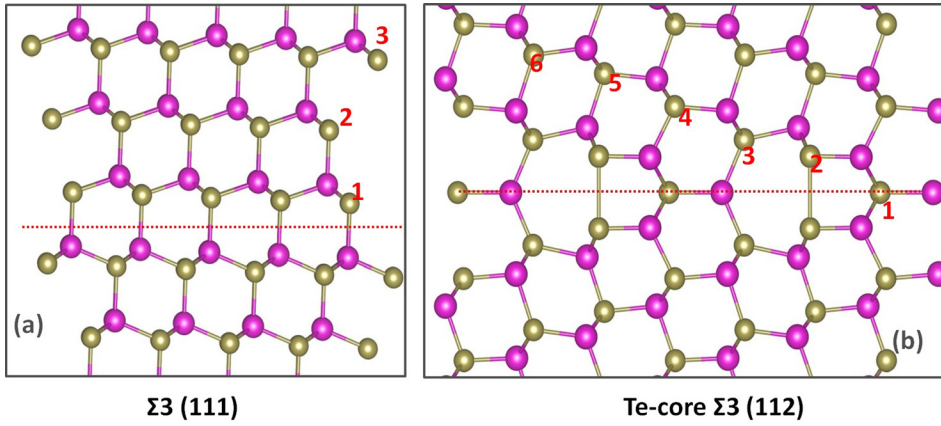


FIG. 1. Two CdTe grain boundaries used in this work. (a) $\Sigma 3(111)$ GB without wrong bonds and (b) Te-core $\Sigma 3(112)$ GB with the Te-Te wrong bonds. Pink balls are Cd atoms and brown balls are Te atoms. The numbers in the figures are layer numbers away from the GB cores, which are used to describe the Cu and Cl sites in Figs. 5 and 6.

a 64-atom supercell where all the atoms in the supercell are fully relaxed until the forces on every atom are less than 0.05 eV/Å. The total energy is calculated with a $2 \times 2 \times 2$ Monkhorst-Pack special k-point mesh and the Gaussian smearing method (SIGMA = 0.02) to ensure that it converges to within 0.1 eV using an energy cutoff of 300 eV. The defect formation energy $\Delta H_f(\alpha, q)$ as a function of the electron Fermi energy E_F and the atomic chemical potentials μ_i is given by²⁷

$$\Delta H_f(\alpha, q) = \Delta E(\alpha, q) + \sum n_i \mu_i + qE_F, \quad (1)$$

where $\Delta E(\alpha, q) = E(\alpha, q) - E(\text{CdTe}) + n_i E(i) + qE_{VBM}$, E_F is referenced to the VBM of bulk CdTe, and μ_i is the chemical potential of constituent i referenced to elemental solid or gas with energy $E(i)$. The n 's are the numbers of atoms taken out of the supercell to form the defects, and q is the number

of electrons transferred from the supercell to the Fermi reservoirs in forming the defect cell. The defect transition energy level $\varepsilon_\alpha(q/q')$ is the Fermi energy E_F in Eq. (1) at which the formation energy $\Delta H_f(\alpha, q)$ of defect α at charge q is equal to that of the same defect at another charge state q' , i.e.,

$$\varepsilon_\alpha(q/q') = [\Delta E(\alpha, q) - \Delta E(\alpha, q')]/(q' - q). \quad (2)$$

For GB calculations, we used two typical and most energetically favorable GB configurations^{28–31} as shown in Fig. 1, i.e., $\Sigma 3(111)$ GBs and Te-core $\Sigma 3(112)$ GBs.³¹ The segregations of Cu and Cl at GBs are calculated using the generalized gradient approximation (GGA) formulated by Perdew, Burke, and Ernzerhof (PBE)³² due to the large system size, and the segregation energy is defined as the total energy difference when Cu or Cl atom is put at the GB cores and at sites far from the GB cores.

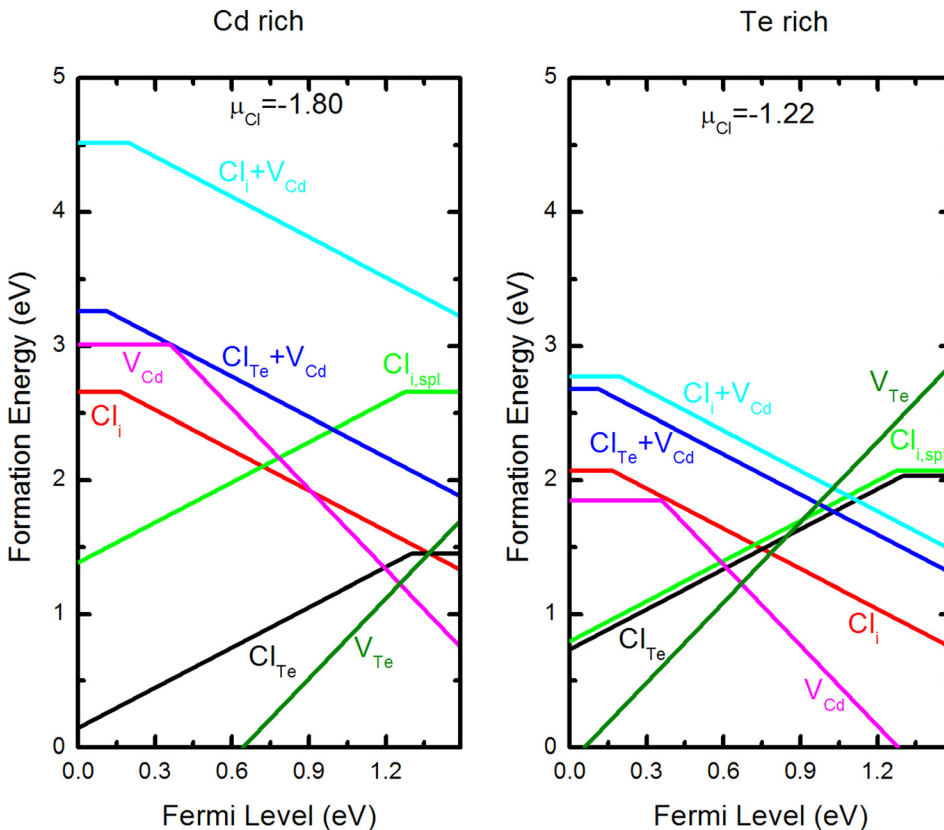


FIG. 2. Cl-related defect formation energies in bulk CdTe as functions of Fermi levels under (a) Cd rich conditions and (b) Te rich conditions. The chemical potential conditions are $\mu_{Cd} + \mu_{Te} = -1.17$ eV and $\mu_{Cd} + 2\mu_{Cl} < -3.60$ eV. Note that for Cl interstitials, red lines and green lines are used to stand for (0/-) and (0/+) transitions, respectively. The defect transition energy levels are those turning points.

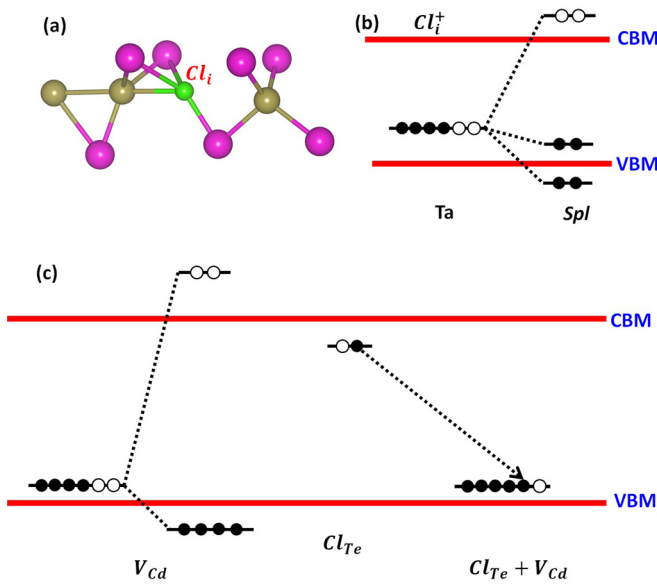


FIG. 3. (a) Most stable structure of Cl_i^+ , where Cl forms a bond with Te. This kind of structure is named as *Spl* structure and pink balls are Cd atoms, brown balls are Te atoms, and green balls are Cl atoms. (b) Diagrams to show how *Spl* structure is stabilized by level splitting. (c) Diagrams to show how neutral Cd vacancy is stabilized by level splitting and how A center forms shallow acceptor level in bulk CdTe.

III. RESULTS AND DISCUSSIONS

First, let us discuss Cl doping in bulk CdTe. We find that Cl can either substitute Te atoms to form Cl_{Te} or form interstitial defects. Because Cl has one more electron than Te, Cl_{Te} is expected to be a donor, with a calculated (0/+) transition energy level of 0.19 eV below the conduction band minimum (CBM), as shown in Fig. 2. Cl

interstitial defects are more complex. For the neutral interstitial, Cl is found to be most stable at the Bc site (middle between two neighboring cations) in Ref. 33 due to level splitting caused by reduced symmetry. For the -1 charged interstitial, Cl is stabilized at the center of the tetrahedron surrounded by four Cd (Tc site), as expected. In this case, Cl interstitial behaves as a shallow acceptor with a (0/−) transition energy level of 0.17 eV above the VBM. However, when the Cl interstitial is positively charged, we find that there is competition between lattice distortions and electron level splitting. Positively charged Cl interstitial can gain high Coulomb energy at the center of the tetrahedron surrounded by four negatively charged Te ions (Ta site). In the distorted *Spl* structure, the Cl interstitial forms a Cl-Te bond at Te site, as shown in Fig. 3(a). Due to the structure distortion, the electron levels are split and the Cl interstitial can have a large electronic energy gain, as shown in Fig. 3(b), which is similar to the behavior of neutral Te interstitial in Ref. 33. Because the electronic energy gain due to level splitting is larger than the energy cost to have such structure distortion, the positively charged Cl interstitial is found most stable at *Spl* site. In this case, Cl interstitial will act as a donor with a (0/+) level of 0.22 eV below the CBM.

Beside the point defects, Cl can also form a defect complex such as the A center ($Cl_{Te} + V_{Cd}$). When the A center forms, the additional electron of Cl_{Te} will spontaneously fill the empty defect state of Cd vacancy. Initially, the neutral Cd vacancy has two holes, which leads to large structural distortions and level splitting, resulting in a relatively deep negative U (0/2−) acceptor level at 0.36 eV above the VBM as explained in Ref. 34 and shown in Fig. 3(c). When Cl_{Te} is present near Cd vacancy, charge transfer from Cl_{Te} to V_{Cd}

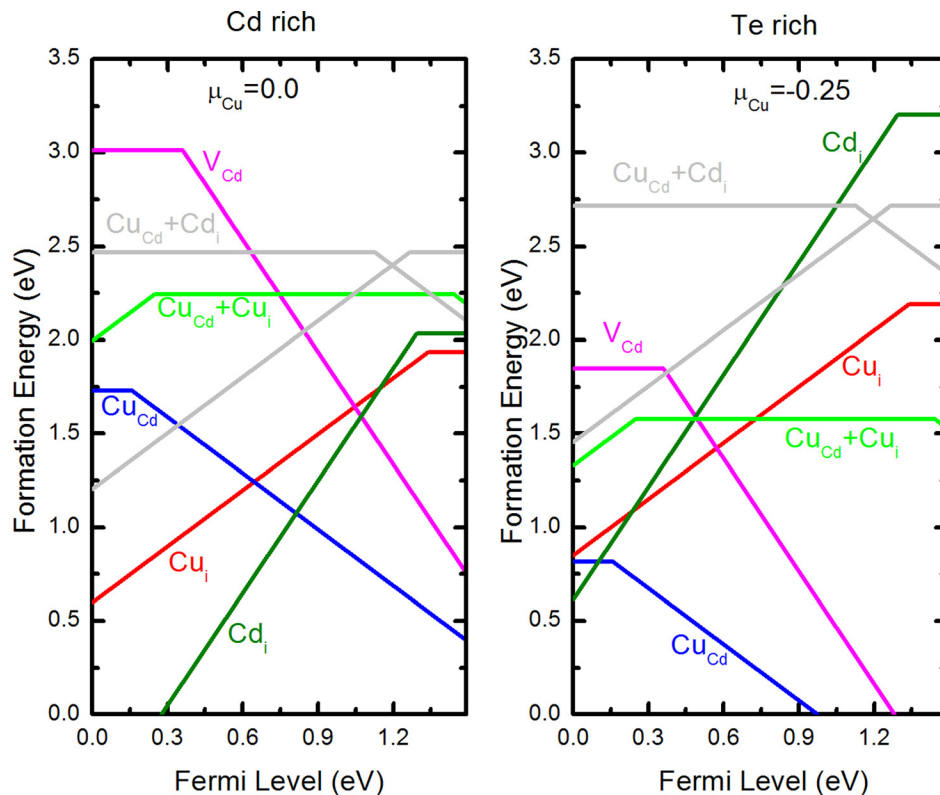


FIG. 4. Cu-related defect formation energies in bulk CdTe as functions of Fermi levels under (a) Cd rich conditions and (b) Te rich conditions. The chemical potentials conditions are $\mu_{Cd} + \mu_{Te} = -1.17$ eV and $\mu_{Cu} + \mu_{Te} < -0.25$ eV. The defect transition energy levels are those turning points.

will occur and make the structural distortion of the Cd vacancy not energetically favored. As a result, the A center has a shallow ($0/-$) acceptor level of about 0.11 eV above the VBM, in agreement with the experimental result.³⁵ In this sense, the A center indeed can improve p-type doping in bulk CdTe. However, the concentration of the A center will be limited by the concentration of Cd vacancies. Once the Cd vacancies are all consumed, the A center will have a higher formation energy than Cl interstitials and Cl_{Te} . The consequence is that negatively charged Cl interstitials will compensate the positively charged Cl interstitials and Cl_{Te} ,

pinning the Fermi level in the middle of bandgap and leading to deep levels in Cl doped bulk CdTe, as shown in Fig. 2. Our calculated results can be compared with the experimental results in Refs. 8 and 12, which indicate that too much Cl incorporation into bulk CdTe can be harmful.

For Cu doping in bulk CdTe, it can form two important defects. One is the substitutional defect Cu_{Cd} and the other is Cu interstitial. Because Cu has one valance electron less than Cd, Cu_{Cd} behaves as an acceptor. Due to the anion p -Cu d coupling effect in tetragonal semiconductors, Cu substitutions usually have deep acceptor levels.³⁶ However, in CdTe,

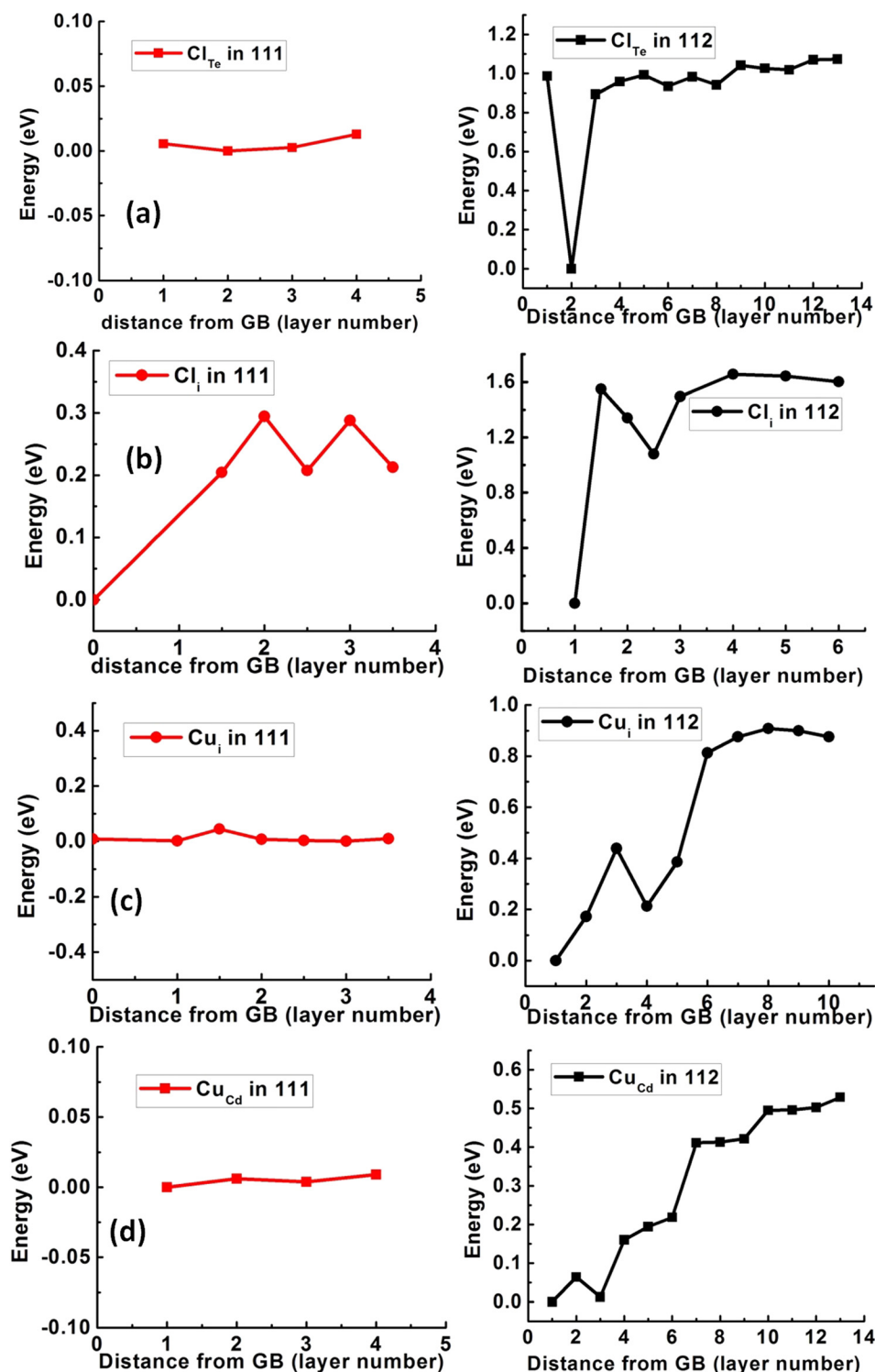


FIG. 5. Segregation of charge neutral Cu and Cl defects at GBs. (a) Cl_{Te} , (b) Cl_i , (c) Cu_i , and (d) Cu_{Cd} segregations at $\Sigma 3(111)$ and Te-core $\Sigma 3(112)$ GBs, respectively. The lowest energy points are set as zero, the layer numbers are labeled in Fig. 1, and the structural configurations are shown in Fig. 7.

p-d coupling is strongly suppressed because of the large lattice constant. As a result, Cu_{Cd} in bulk CdTe has a relatively shallow (0/−) acceptor level of 0.16 eV above the VBM, as shown in Fig. 4. Our HSE06 result differs slightly from the previous calculation³⁷ based on local density approximation (LDA) because a supercell size correction of about 0.06 eV is used in current calculation. Experimentally, this level varies between 0.15 eV and 0.35 eV.^{20,38–42} However, compared with the recently calculated acceptor level of Cd vacancy,^{34,43} which is about 0.36 eV above the VBM, Cu_{Cd} (0/−) level is much

shallower. As a result, Cu doping in bulk CdTe should be able to improve the p-type conductivity, as observed experimentally.^{15,16} What is more, under Te rich conditions, Cu substitution defect always has lower formation energy than Cu interstitial (see Fig. 4). Thus, the dopant self-compensation can be suppressed by properly controlling the growth conditions. Although the Cu_{Cd} level is still relatively deep compared with acceptor levels in other solar cell materials such as CuInSe_2 and $\text{Cu}_2\text{ZnSnS}_4$, Cu is the best cation-substituting acceptor up to now. To make acceptor level closer to the

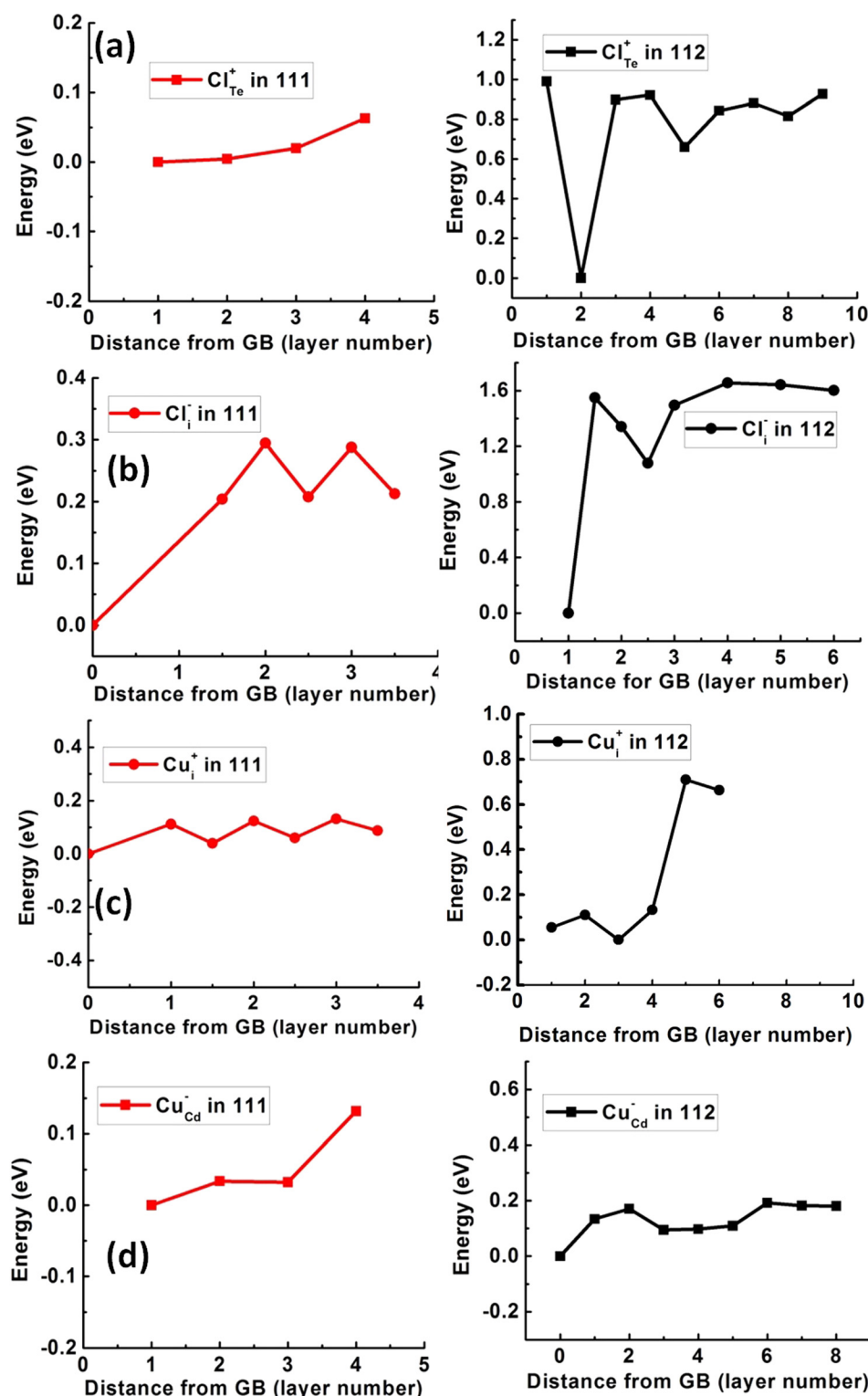


FIG. 6. Segregation of charged Cu and Cl defects at GBs. (a) Cl_{Te}^+ , (b) Cl_i^- , (c) Cu_i^+ , and (d) Cu_{Cd}^- segregations at $\Sigma 3(111)$ and Te-core $\Sigma 3(112)$ GBs, respectively. The lowest energy points are set as zero, the layer numbers are labeled in Fig. 1, and the structural configurations are shown in Fig. 7.

VBM, anion-substituting acceptors such as P_{Te} and As_{Te} have to be considered.⁴⁴ However, the latter also has problems such as the formation of AX centers and high-efficiency CdTe solar cells based on anion doping are still under development. More importantly, besides p-type doping, Cu also plays an important role in forming the low resistance back contacts, although Cu also induces stability problems due to its fast diffusion in bulk CdTe.^{33,45–47}

Now that we have clarified the Cl and Cu-related defects in bulk CdTe, we turn to discuss their behaviors at GBs. We want to point out that the defect behaviors at GBs might vary with different GB structures. Here, we focus our study on the two typical and most energetically favorable GBs, $\Sigma 3(111)$ and $\Sigma 3(112)$ GBs, as shown in Fig. 1. The $\Sigma 3(111)$ GB can be seen as a stacking fault between the zinc-blende and wurtzite structures. Because there are no dangling bonds and wrong bonds in $\Sigma 3(111)$ GB, its formation energy is very low and this GB is expected to have large populations in polycrystalline CdTe.³¹ The Te-core $\Sigma 3(112)$ GB, on the other hand, contains Te-Te wrong bonds, which form deep gap states and be harmful for CdTe electronic properties. Because this GB also has relatively low formation energy compared with other GBs, Te-core $\Sigma 3(112)$ GB is expected to exist in significant amounts.

Figs. 5 and 6 show our calculated results in these two GBs. In general, Cu and Cl show little segregation at $\Sigma 3(111)$ GBs as expected from the similarity between this GB and bulk, except that the Cl interstitial has segregation

energy of about 0.2 eV. This is because the stacking fault at $\Sigma 3(111)$ GBs gives the Cl interstitial more space to occupy, as shown in Fig. 7(a). On the other hand, the energy of the neutral Cu interstitial does not depend sensitively on the space but depends on the s - d coupling.^{33,45} As a result, the Cu interstitial does not show segregation at $\Sigma 3(111)$ GBs.

The findings are different for the Te-core $\Sigma 3(112)$ GB. For Cl interstitial, the Te-core $\Sigma 3(112)$ GB offers Cl interstitial increased space as shown in Fig. 7(b) and as a result, the segregation energy of Cl interstitial is as large as 1.2 eV for both neutral and charged states. For Cl substitution, because the Te-Te wrong bond is broken due to the smaller size of Cl [Fig. 7(c)], each Te dangling bond state will relax back into valence band. As each Te dangling bond has 1.5 electrons (see Ref. 7), Cl will transfer 0.5 electrons to each Te and passivate the dangling bond. Consequently, there exists a large energy gain, resulting in the strong segregations of Cl_{Te} . When Cl_{Te} is +1 charged, charge transfer can still happen from the VBM of CdTe to the Te dangling bond, resulting in a smaller but still large energy gain, as seen in Figs. 5(a) and 6(a). Consequently, Cl_{Te}^+ also shows relatively strong segregation. Our results are consistent with the experimental observations^{8–11} and previous studies.⁷

Similarly, for neutral Cu interstitials, Cu sits near the middle of Te-Te bond [see Fig. 7(e)], thus breaking Te-Te state. The extra one electron of Cu interstitial transfers to the two Te dangling bonds, resulting in a large energy gain and strong segregation of neutral Cu interstitials at the

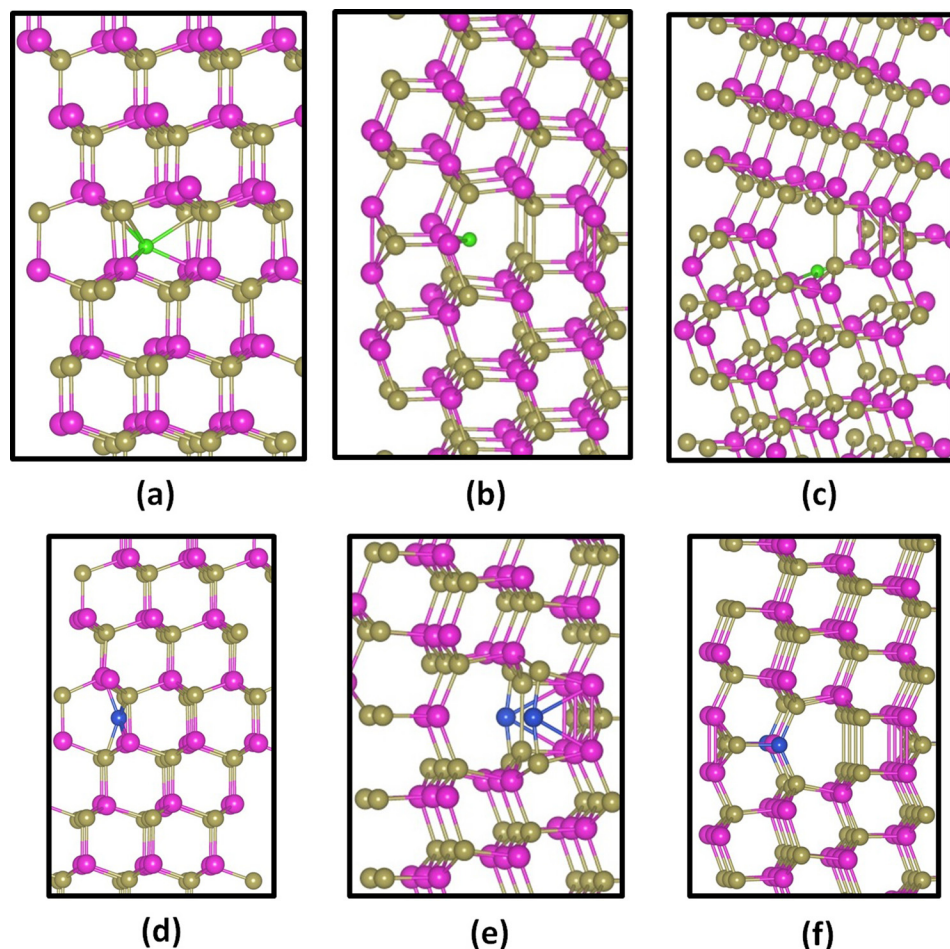


FIG. 7. Structural configurations of Cu and Cl defects at CdTe GBs. (a) Cl interstitial at $\Sigma 3(111)$ GB. (b) Cl interstitial at Te-core $\Sigma 3(112)$ GB. (c) Cl substitution at Te-core $\Sigma 3(112)$ GB. (d) Cu interstitial at $\Sigma 3(111)$ GB. (e) Cu interstitial at Te-core $\Sigma 3(112)$ GB. (f) Cu substitution at Te-core $\Sigma 3(112)$ GB. Pink balls are Cd atoms, brown balls are Te atoms, green balls are Cl atoms, and blue balls are Cu atoms.

Te-core $\Sigma 3(112)$ GB. When Cu interstitial becomes positively charged, charge transfer from the VBM of CdTe to the Te dangling bonds still cause the segregation of Cu interstitials. For Cu substitutions at Te-core $\Sigma 3(112)$ GB [Fig. 7(f)], the segregation of neutral defect can be explained as follows. Because Cu_{Cd} can introduce a partially occupied acceptor state close to the VBM, the occupied Te-Te antibonding state can transfer one electron to the acceptor state with an energy gain. However, when Cu_{Cd} is negatively charged, the acceptor state is now fully occupied and there is no charge transfer from the Te-Te state anymore. As a result, after Cu_{Cd} is negatively charged, the segregation of Cu_{Cd} is strongly suppressed. We notice that Cu segregation is reported experimentally,^{16,48,49} which can be owed to Cu interstitials or neutral Cu on Cd sites at Te-core $\Sigma 3(112)$ GBs.

VI. CONCLUSIONS

In conclusion, we have systematically studied the Cu and Cl-related defects in polycrystalline CdTe. We find that while Cl has a limited effect on improving p-type doping in the bulk region, too much Cl will have a negative effect. Cu can help to improve p-type doping of bulk CdTe. In the presence of GBs, we found Cl and Cu will prefer to stay at GBs, especially those with Te-Te wrong bonds, in agreement with the experimental observations. Our work, therefore, provides a better understanding of Cu and Cl effects in polycrystalline CdTe.

ACKNOWLEDGMENTS

This work was funded by the U.S. Department of Energy, EERE/SunShot program, under Contract No. DE-AC36-08GO28308. The calculations are done on peregrine supercomputer and NERSC supercomputer.

- ¹M. A. Green, K. Emery, Y. Hishikawa, W. Warta, and E. D. Dunlop, *Prog. Photovoltaics* **23**, 805 (2015).
- ²H. R. Moutinho, M. M. Al-Jassim, D. H. Levi, P. C. Dippo, and L. L. Kazmerski, *J. Vac. Sci. Technol., A* **16**, 1251 (1998).
- ³B. E. McCandless, L. V. Moulton, and R. W. Birkmire, *Prog. Photovoltaics* **5**, 249 (1997).
- ⁴W. K. Metzger, D. Albin, M. J. Romero, P. Dippo, and M. Young, *J. Appl. Phys.* **99**, 103703 (2006).
- ⁵M. Terheggen, H. Heinrich, G. Kostorz, A. Romeo, D. Baetzner, A. N. Tiwari, A. Bosio, and N. Romeo, *Thin Solid Films* **431**, 262 (2003).
- ⁶V. Komin, B. Tetali, V. Viswanathan, S. Yu, D. L. Morel, and C. S. Ferekides, *Thin Solid Films* **431**, 143 (2003).
- ⁷L. Zhang, J. L. F. Da Silva, J. Li, Y. Yan, T. A. Gessert, and S.-H. Wei, *Phys. Rev. Lett.* **101**, 155501 (2008).
- ⁸S. A. Ringel, A. W. Smith, M. H. MacDougall, and A. Rohatgi, *J. Appl. Phys.* **70**, 881 (1991).
- ⁹I. Visoly-Fisher, S. R. Cohen, K. Gartsman, A. Ruzin, and D. Cahen, *Adv. Funct. Mater.* **16**, 649 (2006).
- ¹⁰I. Visoly-Fisher, S. R. Cohen, A. Ruzin, and D. Cahen, *Adv. Mater.* **16**, 879 (2004).
- ¹¹C. Li, Y. Wu, J. Poplawsky, T. J. Pennycook, N. Paudel, W. Yin, S. J. Haigh, M. P. Oxley, A. R. Lupini, M. Al-Jassim, S. J. Pennycook, and Y. Yan, *Phys. Rev. Lett.* **112**, 156103 (2014).
- ¹²A. Castaldini, A. Cavallini, B. Fraboni, P. Fernandez, and J. Piqueras, *J. Appl. Phys.* **83**, 2121 (1998).
- ¹³D. H. Rose, F. S. Hasoon, R. G. Dhere, D. S. Albin, R. M. Ribelin, X. S. Li, Y. Mahathongdy, T. A. Gessert, and P. Sheldon, *Prog. Photovoltaics* **7**, 331 (1999).
- ¹⁴E. I. Adirovich, Yu. M. Yuabov, and G. R. Yagudaev, *Sov. Phys. - Semicond.* **3**, 61 (1969).
- ¹⁵L. Kranz, C. Gretener, J. Perrenoud, R. Schmitt, F. Pianezzi, F. L. Mattina, P. Blösch, E. Cheah, A. Chirilă, C. M. Fella, H. Hagendorfer, T. Jäger, S. Nishiwaki, A. R. Uhl, S. Buecheler, and A. N. Tiwari, *Nat. Commun.* **4**, 2306 (2013).
- ¹⁶J. Perrenoud, L. Kranz, C. Gretener, F. Pianezzi, S. Nishiwaki, S. Buecheler, and A. N. Tiwari, *J. Appl. Phys.* **114**, 174505 (2013).
- ¹⁷T. A. Gessert, W. K. Metzger, P. Dippo, S. E. Asher, R. G. Dhere, and M. R. Young, *Thin Solid Films* **517**, 2370 (2009).
- ¹⁸C. R. Corwine, A. O. Pudov, M. Gloeckler, S. H. Demtsu, and J. R. Sites, *Sol. Energy Mater. Sol. Cells* **82**, 481 (2004).
- ¹⁹D. S. Albin, "Accelerated stress testing and diagnostic analysis of degradation in CdTe solar cells," *Proc. SPIE* **7048**, 70480N (2008).
- ²⁰J. P. Chamonal, E. Molva, and J. L. Pautrat, *Solid State Commun.* **43**, 801 (1982).
- ²¹P. Hohenberg and W. Kohn, *Phys. Rev.* **136**, B864 (1964).
- ²²W. Kohn and L. J. Sham, *Phys. Rev.* **140**, A1133 (1965).
- ²³G. Kresse and J. Furthmüller, *Phys. Rev. B* **54**, 11169 (1996).
- ²⁴G. Kresse and J. Furthmüller, *Comput. Mater. Sci.* **6**, 15 (1996).
- ²⁵G. Kresse and D. Joubert, *Phys. Rev. B* **59**, 1758 (1999).
- ²⁶J. Heyd, G. E. Scuseria, and M. Ernzerhof, *J. Chem. Phys.* **118**, 8207 (2006).
- ²⁷S.-H. Wei, *Comput. Mater. Sci.* **30**, 337 (2004).
- ²⁸Y. Yan, M. M. Al-Jassim, K. M. Jones, S.-H. Wei, and S. B. Zhang, *Appl. Phys. Lett.* **77**, 1461 (2000).
- ²⁹Y. Yan, M. M. Al-Jassim, and K. M. Jones, *J. Appl. Phys.* **94**, 2976 (2003).
- ³⁰C. Sun, N. Lu, J. Wang, J. Lee, X. Peng, R. F. Klie, and M. J. Kim, *Appl. Phys. Lett.* **103**, 252104 (2013).
- ³¹J.-S. Park, J. Kang, J.-H. Yang, W. Metzger, and S.-H. Wei, *New J. Phys.* **17**, 013027 (2015).
- ³²J. P. Perdew, K. Burke, and M. Ernzerhof, *Phys. Rev. Lett.* **77**, 3865 (1996).
- ³³J. Ma, J. Yang, S.-H. Wei, and J. L. F. Da Silva, *Phys. Rev. B* **90**, 155208 (2014).
- ³⁴J.-H. Yang, J.-S. Park, J. Kang, W. Metzger, T. Barnes, and S.-H. Wei, *Phys. Rev. B* **90**, 245202 (2014).
- ³⁵D. M. Hofmann, D. Omling, H. G. Grimmeiss, B. K. Meyer, K. W. Benz, and D. Sinerius, *Phys. Rev. B* **45**, 6247 (1992).
- ³⁶Y. Yan, M. M. Al-Jassim, and S.-H. Wei, *Appl. Phys. Lett.* **89**, 181912 (2006).
- ³⁷S.-H. Wei and S. B. Zhang, *Phys. Rev. B* **66**, 155211 (2002).
- ³⁸A. Balcioğlu, R. K. Ahrenkiel, and F. Hasoon, *J. Appl. Phys.* **88**, 7175 (2000).
- ³⁹A. A. Gippius, J. R. Panossian, and V. A. Chapnin, *Phys. Status Solidi A* **21**, 753 (1974).
- ⁴⁰F. A. Kröger, *Rev. Phys. Appl. (Paris)* **12**, 205 (1977).
- ⁴¹A. S. Gilmore, V. Kaydanov, and T. R. Ohno, "The study of deep levels in CdS/CdTe solar cells using admittance spectroscopy and its modifications," *MRS Proc.* **763**, B9.6 (2003).
- ⁴²M. Said and M. A. Kanehisa, *J. Cryst. Growth* **101**, 488 (1990).
- ⁴³J. Ma, D. Kuciauskas, D. Albin, R. Bhattacharya, M. Reese, T. Barnes, J. V. Li, T. Gessert, and S.-H. Wei, *Phys. Rev. Lett.* **111**, 067402 (2013).
- ⁴⁴J.-H. Yang, W.-J. Yin, J.-S. Park, J. Burst, W. K. Metzger, T. Gessert, T. Barnes, and S.-H. Wei, *J. Appl. Phys.* **118**, 025102 (2015).
- ⁴⁵J. Ma and S.-H. Wei, *Phys. Rev. Lett.* **110**, 235901 (2013).
- ⁴⁶E. D. Jones, N. M. Stewart, and J. B. Mullin, *J. Cryst. Growth* **117**, 244 (1992).
- ⁴⁷H. H. Woodbury and M. Aven, *J. Appl. Phys.* **39**, 5485 (1968).
- ⁴⁸D. L. Baetzner, A. Romeo, H. Zogg, R. Wendt, and A. N. Tiwari, *Thin Solid Films* **387**, 151 (2001).
- ⁴⁹K. D. Dobson, I. Visoly-Fisher, G. Hodes, and D. Cahen, *Sol. Energy Mater. Sol. Cells* **62**, 295 (2000).